International Journal of Mechanical Sciences 215 (2022) 106962

Contents lists available at ScienceDirect

International Journal of Mechanical Sciences

journal homepage: www.elsevier.com/locate/ijmecsci

Star-shaped piezoelectric mechanical energy harvesters for multidirectional sources

Virgilio J. Caetano, Marcelo A. Savi *

Department of Mechanical Engineering, Center for Nonlinear Mechanics, COPPE, Universidade Federal do Rio de Janeiro, P.O. Box 68503, Rio de Janeiro 21941-972, Brazil

ARTICLE INFO

Keywords:
Energy harvesting
Multimodal harvester
Multidirectional harvester
Piezoelectric
Finite element analysis
ANSYS

ABSTRACT

This work deals with multidirectional and multimodal piezoelectric mechanical energy harvesters, proposing a star-shaped device composed by a tri-leg *L*-shaped structure with piezoelectric patches at six locations. Inertial pendular masses are strategically attached to the structure to harvest energy due to three-direction excitation sources. The device is modeled using finite element method and simulations are carried out to optimize the system design to operate in the required frequency range. System performance is investigated considering different ambient conditions including random excitations that represent the unavoidable source uncertainties. Results for in-plane and out-of-plane excitations show that the proposed device has potential to extract energy from multidirectional sources with a wideband frequency spectrum, serving as an alternative to conventional single-mode harvester with unidirectional sensitivity.

1. Introduction

Electronic devices have been continuously evolving in recent decades, with a continuous need of energy. Some applications employ wireless microelectronics that require their own power supply. Internet of things is an emblematic example where energy needs to be provided for isolated areas. Nevertheless, there are several other applications related to aerospace technology and oil & gas industry. All these aspects motivate the harness of available ambient energy that, otherwise, would be wasted.

Piezoelectric energy harvesting from ambient sources, especially mechanical vibration-based ones, has gathered considerable focus as a promising solution to portable self-powered electronic devices due to their structural simplicity, compatibility, and high conversion capacity. The most common vibration-based energy harvester configurations are the piezoelectric beams [14,20,21,26]. Several works based on cantilever beam models have been numerically investigated and experimentally tested through piezoelectric linear devices [3–7]. These devices are modeled as linear mechanical oscillators connected to an electronic circuit through a piezoelectric electromechanical coupling. Results show that these devices present interesting behavior under resonant conditions, losing performance when the excitation frequency is distributed over a broader range. Despite the advantages of simplicity and high-power density, linear harvesters have the drawback of narrow bandwidth and unidirectional sensitivity, being suitable for stationary excitations with narrowband near natural frequency. These aspects may limit the use of energy harvesters to applications where the ambient excitation is distributed across a wide spectrum and various directions.

These drawbacks encouraged a variety of strategies to broaden the bandwidth and enhance the performance of the linear energy harvesters, incorporating nonlinearities, active or passive adaptative frequency-tuning methods, oscillator arrays, multimodal systems, among others [31,42].

One possible approach to widen the frequency bandwidth of the harvesters consists of using multiple-degrees-of-freedom (MDoF) systems, including an array of structures or coupled oscillators, as discussed in Kim et al. [15], Tang and Yang [29] and Wu et al. [35]. A simple concept is to integrate multiple cantilever beams with tip masses, modeled as single-degree-of-freedom (SDoF) oscillators with different natural frequencies, increasing the effective operating frequency range [11,23,25]. This approach is usually related to the increase of either the energy harvester size or the electric circuit complexity. Multimodal energy harvesters constitute an interesting alternative where different oscillators can be coupled together, producing a wider frequency bandwidth.

Several works have been done proposing devices that improve the

* Corresponding author.
E-mail address: savi@mecanica.coppe.ufrj.br (M.A. Savi).

https://doi.org/10.1016/j.ijmecsci.2021.106962
Received 30 July 2021; Received in revised form 5 November 2021; Accepted 22 November 2021
Available online 24 November 2021

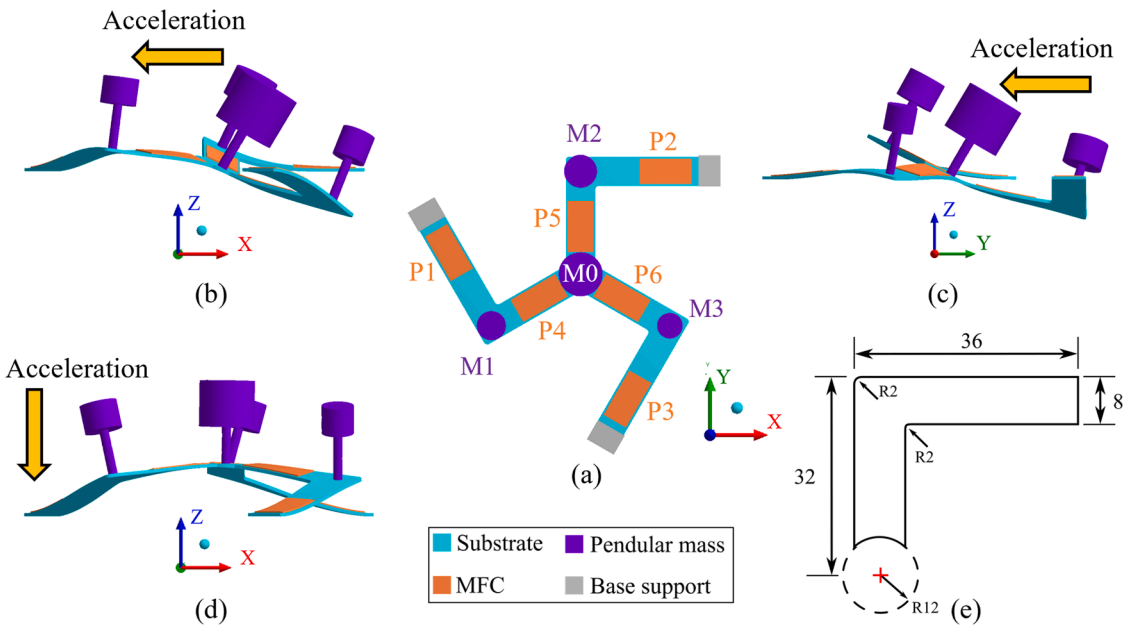

Fig. 1. Schematic picture of the multidirectional star-shaped (MSS) energy harvester: (a) frontal view; (b) device under acceleration in *x*-axis direction; (c) device under acceleration *y*-axis direction; (d) device under acceleration *z*-axis direction; (e) dimensions of one *L*-shaped leg.

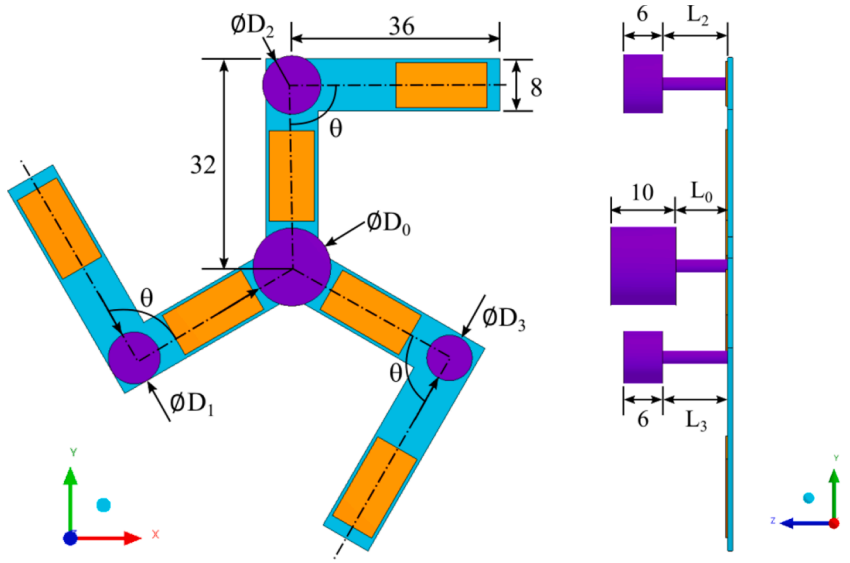

Fig. 2. Frontal and lateral view of MSS energy harvesting device with dimensions in mm, showing the parameters used in the optimization procedure.

system performance concerning the generated energy and broader bandwidth. Systems with two-degrees-of-freedom [15,28,29,30,37] and three-degree-of-freedom [17,18,32] have been designed in order to present close resonant peaks, expanding the operational frequency range. These harvesters exploit geometrical and mechanical characteristics including inertial, elastic, and magnetic coupling to carefully tune resonant frequencies, expanding the frequency bandwidth.

The nonlinear exploitation is another strategy to enhance the energy harvesting performance [19,[23,24],38]. Magnetic interaction is a common technique employed in piezoelectric energy harvesters (PEH), defining different stability properties as bistable and tristable systems [12]. Erturk et al. [4–8] investigated nonlinear piezo-magneto-elastic energy harvesters that exhibit vibration of low and high-energy orbits showing significant improvement with respect to the bandwidth and the performance over traditional linear piezo-elastic energy harvester. Instead of employing fixed external magnets, some studies are focused on adjustable or movable magnets to further enhance the system performance [16,34]. Multistable energy harvesters [41], including tristable [22,33] and quad-stable [39,40] systems, have been investigated as alternatives to reduce the potential barrier of bistable systems, benefiting energy harvesting associated with low-amplitude excitation conditions keeping the broadband capability.

Although MDoF nonlinear systems expand the energy harvester operational bandwidth, most of them are still associated with unidirectional behavior, usually suitable for operating under transverse vibration direction. Real-world applications are associated with ambient mechanical vibration spread over a wider frequency spectrum that comes from various directions, such as ocean waves, wind, and human motion. In this regard, it is noticeable that few scientific efforts have been carried out to treat energy harvester subjected to multidirectional and broad bandwidth excitations [9,10,13,27,36]. Su and Zu [27] proposed a PEH system composed of three sub-systems that utilize magnets

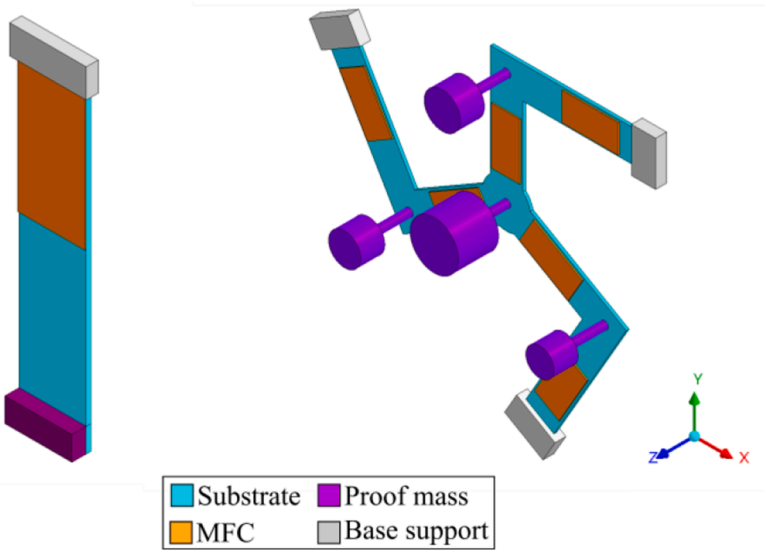

Fig. 3. Isometric view of the cantilever-beam (left-side) and the original MSS (right-side) energy harvesting devices.

Table 1
Geometric dimensions and material properties of the MSS energy harvester.

Parameter	Substrate	Piezoelectric	Tip Mass
Material	Aluminum	MFC0714-P2	Steel
Density (kg/m^3)	2700	5440	7850
Elastic modulus (GPa)	69	30.336	200
Poisson ratio	0.33	0.3	0.3
Length (mm) × width (mm) × thickness (mm)	64 × 8 × 1	7 × 14 × 0.3	–
Piezoelectric constant: e_{31} (C/m^2)	–	− 5.16	–
Relative permittivity	–	1900	–
Permittivity constant (pF/m)	–	8.854	–
Modal damping ratio	$\xi = 0.02$		

to introduce nonlinear force, coupled to permit the extraction of vibration energy from three directions and over a broad bandwidth. Yu et al [36] investigated the vibro-impact mechanism between a spiral cylindrical spring system and multi-piezoelectric-beams to harness energy from three-directional vibration excitations. These harvesters present a broadband spectrum that is related to nonlinearities characterized by a region with the coexistence of low and high-energy orbits. Nevertheless, the bandwidth gain assumes that the system operates associated with high-energy orbits that would require a controller to maintain the efficiency of the harvester operation. Fattahi and Mirdamadi [9,10] proposed a novel 3D skeletal frame energy harvester for multidirectional excitation that explores structure asymmetries to solve the shortcoming of multimodality, obtaining wider bandwidth. Another interesting approach is proposed by Hung et al. [13] that employed an inertial pendular mass to convert three-axis vibration energy into electricity using four piezoelectric beams. Although the harvester provides multidirectional sensitivity, being interesting for extracting energy from different direction excitations, the system presents narrow frequency bandwidth characterized by a single mode which would lose performance for wideband excitations.

Based on these aspects, it is relevant to develop novel energy harvester designs that can offer better performance concerning multimodal and multidirection excitations. This work deals with the development of a novel design configuration for multidirectional and multimodal piezoelectric mechanical energy harvesting device. The harvester conception and optimization is investigated, proposing a star-shaped (MSS) device composed of a tri-leg structure with inertial pendular masses strategically positioned in the structure to extract energy from three-directions. An optimization procedure based on finite element analysis is developed using ANSYS software, allowing one to adjust multiple resonant frequencies within a desired operational frequency range and establishing suitable performance conditions of the system under different ambient vibration sources. Modal and harmonic analyses are carried out to determine configuration in which the system presents better performance regarding broad bandwidth and generated output power. Random excitations are investigated to represent the unavoidable mechanical vibration source uncertainties. Results show that the proposed configuration is capable of harvesting energy from multidirectional excitation presenting advantages in terms of broadband spectrum compared with conventional linear cantilever beam device.

After this introduction, the paper is organized as follows. Section 2 proposes a multidirectional and multimodal piezoelectric energy harvesting device based on a star-shaped geometry that utilizes inertial pendular masses to allow a multidirectional and broad frequency range behavior. Section 3 presents the mathematical formulation of the finite element analysis for coupled-field piezoelectric problems, including a finite element-based optimization procedure to optimize a multimodal device to set the resonant frequencies in a desired frequency range with close enough resonant peaks in order to extract energy from a wideband spectrum. Section 4 is reserved to the design concept evolution. A comparative analysis with a conventional cantilever beam device is performed to establish the key characteristics of the proposed MSS device. Subsequently, in Section 5, the optimization of the proposed MSS configuration based on geometrical and electrical parameters of the system are carried out. The performance of the energy harvester is investigated considering time history responses to establish the advantage of the system in terms of energy generation from wideband excitations in multiple directions. Random excitations are also investigated. Finally, concluding remarks are discussed.

2. Design configuration

A typical linear vibration energy harvester usually presents some limitations such as unidirectional behavior and narrow operational bandwidth, regardless of the structure and transduction materials. Therefore, multimodal energy harvesters constitute an interesting alternative to increase the operational frequency range by establishing multiple resonant peaks. This work proposes a multimodal, multidirectional star-shaped (MSS) energy harvester device with attached inertial pendular masses (Fig. 1). The goal is to propose, design, and optimize the MSS device to extract energy from wideband ambient vibration in

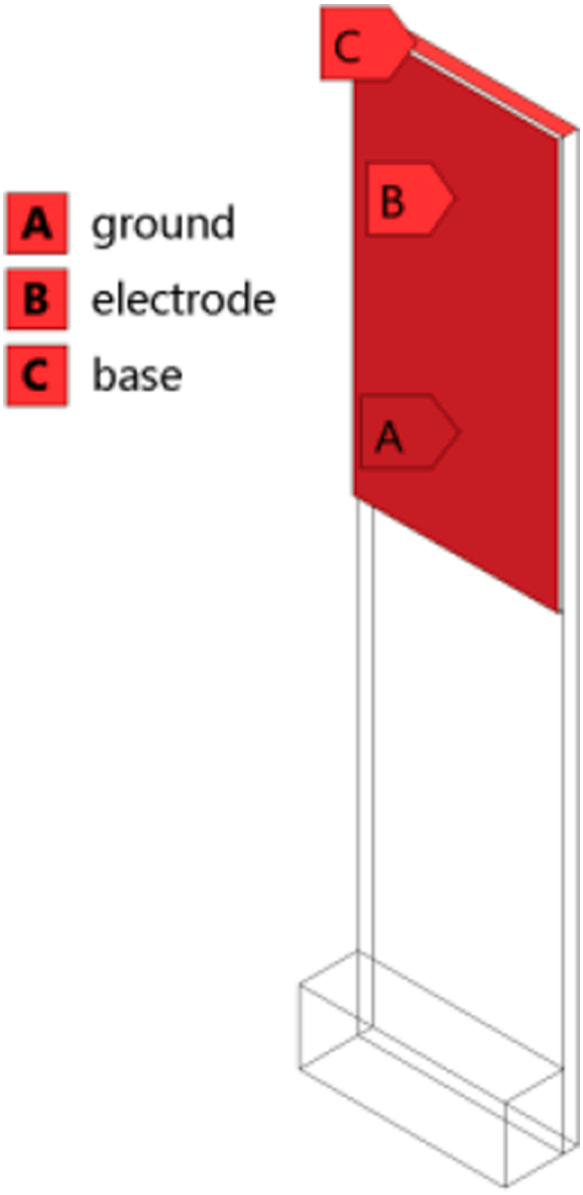

Fig. 4. Schematic representation of the cantilever-type harvester highlighting the electrode and ground (not visible) surfaces of piezoelectric material; and the base surface where the excitation is applied.

three-axis directions. The energy harvester is composed by a substrate, six piezoelectric patches and four inertial pendular masses. The original, pre-optimized configuration consists of three *L*-shaped legs arranged in 120 degrees from each other and connected through one of its ends. Each *L*-shaped leg has two piezoelectric patches and one of its ends is attached to a base support that provides the excitation source. Four inertial pendular masses are strategically connected to the substrate as showed in Fig. 1a.

The harvester is subjected to either in-plane or out-of-plane vibration. Fig. 1b–d present the main characteristics of the excitation effects. Note that excitation applied in the *x*-axis direction, Fig. 1b, or *y*-axis direction, Fig. 1c, makes the pendular masses rotate, promoting deformation of the structure and producing voltage outputs due to the piezoelectric effect. The out-of-plane vibration in the *z*-axis direction is the usual case, also causing the structure deformation, Fig. 1d.

Multimodal systems present frequency response curves characterized by valleys between resonant peaks, related to unavoidable anti-resonant phenomenon, responsible for performance decay in the overall spectrum. The system design needs to mitigate this effect by establishing close resonant peaks, allowing the increase of the harnessing energy efficiently. Another aspect usually employed in the design of energy harvesting systems is the use of tip mass that can provide versatility in tuning the resonant frequencies by carefully changing its weight. In this regard, the inertial pendular masses can be used to provide both multidirectional sensitivity and versatility in tuning the resonant frequencies. In addition, an inertial pendular mass causes higher amplitude oscillations, increasing the strain level on the piezoelectric element and consequently, increasing the generated output power.

The MSS design system performance is compared with a conventional cantilever beam device, showing that the novel design constitutes an evolution toward the goal of broadband and multidirectional energy extraction.

3. Mathematical formulation

Finite element analysis (FEA) is a powerful tool to solve coupled-field problems. Piezoelectric analysis involves bidirectional coupling between structural and electrical fields, respectively represented by a displacement vector, $\{u\}$, and an electrical potential, ϕ. Linear piezoelectric theory can be described by considering T_{ij} as the stress tensor, S_{kl} as the strain tensor; E_k as the electric field vector and D_i as the electrical displacement vector. Therefore, the constitutive equations can be written as follows using indicial notation:

$$\begin{aligned} T_{ij} &= b^E_{ijkl} S_{kl} - e_{kij} E_k \\ D_i &= e_{ikl} S_{kl} + \varepsilon^S_{ik} E_k \end{aligned} \tag{1}$$

where b^E_{ijkl} is the fourth order elastic tensor, ε^S_{ij} is the dielectric second order tensor and e_{ikl} is the third order piezoelectric tensor. The superscripts E and S denote that parameters are evaluated, respectively, at constant electric field and constant stress. After the finite element discretization and application of the variational principle [1], interpolation functions are used to express the continuous displacement and potential in terms of nodal values, resulting in the equation of motion for a single electromechanical element:

$$\begin{bmatrix} [m] & [0] \\ [0] & [0] \end{bmatrix} \begin{Bmatrix} \{\ddot{u}\} \\ \{\ddot{\varphi}\} \end{Bmatrix} + \begin{bmatrix} [c] & [0] \\ [0] & -[c^d] \end{bmatrix} \begin{Bmatrix} \{\dot{u}\} \\ \{\dot{\varphi}\} \end{Bmatrix} + \begin{bmatrix} [k] & [k^c] \\ [k^c]^t & -[k^d] \end{bmatrix} \begin{Bmatrix} \{u\} \\ \{\varphi\} \end{Bmatrix} = \begin{Bmatrix} \{f\} \\ \{q\} \end{Bmatrix} \tag{2}$$

where $[m]$ is the inertia matrix, $[c]$ is the structural damping matrix, $[c^d]$ is the dielectric damping matrix, $[k]$ is the stiffness matrix; $[k^d]$ is the permittivity matrix; $[k^c]$ is the piezoelectric coupling matrix where the subscript $[]^t$ indicates the transpose matrix; $\{f\}$ is the force vector and $\{q\}$ is the electric charge. Details about development of the electromechanical equations of motion based on finite element analysis can be found in Allik and Hughes [1]. By performing a simple nodal addition of element contributions, the equation of motion for a linear structural system with piezoelectric coupling can be rewritten in the compact form.

$$[M]\{\ddot{u}\} + [C]\{\dot{u}\} + [K]\{u\} = \{F\} \tag{3}$$

where $[M]$ is the inertial, $[C]$ is the damping and $[K]$ is the stiffness matrices; $\{F\}$ is the load vector.

The energy harvesters are composed of three structures: substrate, piezoelectric patch and proof mass. ANSYS workbench is employed for numerical simulations and three-dimensional structural elements are employed. Specifically, SOLID186 is employed to model the substrate that is a higher-order 20-nodes element that exhibits quadratic displacement behavior, having three translational degrees-of-freedom per node in the *x*-, *y*- and *z*-directions. Element SOLID226 is employed to model the piezoelectric patches, being similar to the previous one but presenting an additional degree-of-freedom of electric potential for each node. The piezoelectric material uses the d_{31} sensing mode to convert

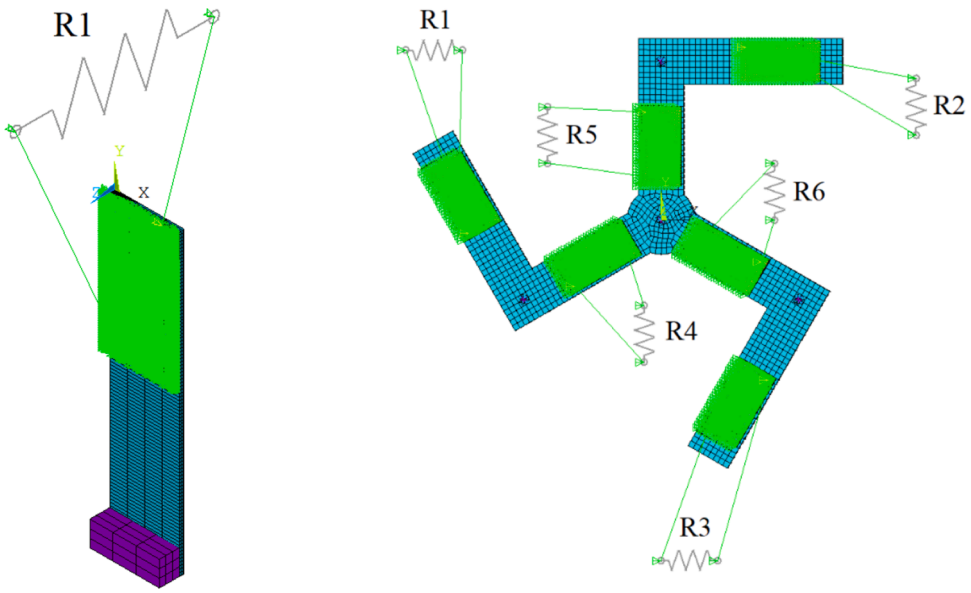

Fig. 5. The cantilever beam and original MSS energy harvesting devices with resistance load, representing the electric circuit, coupled to piezoelectric elements.

bending strain into electric potential. The pendular masses are assumed to be rigid bodies and modeled as point mass elements (MASS21) having three translational DoFs. The electronic circuit is represented by an electric load resistance using element CIRCU94.

Three different types of analysis are developed: modal, harmonic and transient analyses. Modal analysis furnishes the harvester natural frequencies and mode shapes, which are important to determine the frequency range analysis. The harmonic analysis provides the steady-state system response due to a sinusoidal excitation, allowing the coupling of an electric circuit to the piezoelectric patches, which is important to evaluate the generated output power. Finally, transient analysis solves the initial value problem providing the system response for different vibration-based operational conditions.

3.1. Optimization procedure

This section presents an optimization procedure for the MSS piezoelectric harvester based on the idea of converting energy from multidirectional ambient vibration sources with a broadband spectrum. The objective is the design of the multimodal harvester by setting as many resonant frequencies as possible in a desired operational frequency range, mitigating the valleys between resonant peaks and maximizing the generated output power without losing the multidirectional sensitivity characteristic. This is accomplished by minimizing the gap between consecutive natural frequencies and maximizing the area under the output power spectrum, which provides wider bandwidth and more generated energy by unit of frequency in the desired domain.

The operational frequency range of the harvester is defined by a lower limit, ω_L, and an upper limit, ω_U. The optimization considers that p resonant frequencies lay in this desired operational frequency range. The optimization problem is defined as follows by considering a generic frequency ω_j ($j = 1, \ldots, p$) within this interval.

$$\begin{aligned} &\min_{\omega} f_j(\omega) \\ &\text{subject to } g_k^{\omega} \leq 0 \end{aligned} \tag{4}$$

The objective functions $f_j(\omega)$ are defined as follows,

$$\begin{aligned} f_1 &= \omega_1 - \omega_L \\ f_j &= \omega_j - \omega_{j-1} (j = 2, \ldots, p-1) \\ f_p &= \omega_p - \omega_U \\ f_{p+1} &= -\int_{\omega_0}^{\omega_f} P(\omega) d\omega \end{aligned} \tag{5}$$

where $P(\omega)$ is the output power. Note that the last objective function is related to the area under the output power frequency spectrum that needs to be maximized.

The constraints are defined considering a minimal value of variation from consecutive frequencies, ω_g, being written as follows

$$g_k^{\omega} = \omega_g - f_j \leq 0 \quad (k = 1, \ldots, p-1). \tag{6}$$

The optimization procedure is constructed by establishing mechanical and geometric parameters to tune the resonant frequencies, reaching the proposed optimization objectives. It is expected that an increase of the size of L-shaped beams and the weight of pendular masses causes a decrease of the resonant frequencies. Moreover, the length and diameter of pendular masses play an important hole on the harvester multidirectional characteristic. Therefore, resonant frequencies are written as a function of the following parameters: angle between L-shaped beams (θ), diameters (D_0,D_1,D_2,D_3) and length (L_0,L_1,L_2,L_3) of pendular masses, as showed in Fig. 2. In addition, a range for each one of these parameters is defined by lower and upper bound values as follows.

$$\begin{aligned} &\omega_i = \omega_i(\theta, D_l, L_l), \quad (l = 0, \cdots, 3) \quad (i = 1, \cdots, 10) \\ &\text{subject to the constraints :} \\ &\theta_L \leq \theta \leq \theta_U \\ &D_L \leq D_l \leq D_U \end{aligned} \tag{7}$$

The optimization process employs the *Goal-Driven Optimization* (GDO) method based on the Response Surface Optimization (RSO), which can be divided into three main components: Design of Experiments (DOE), Response Surface and Optimization. ANSYS software is employed to perform optimization and Details of the procedure is presented in the sequel [2].

Initially, the model is established by defining geometry and material properties. Afterward, the optimization parameters θ, D_l,L_l ($l = 0, \ldots, 3$) are set as input parameters that have their ranges defined by upper and lower bound values, which determine the design space. Output parameters are used to define optimization objectives and constraints to achieve the design goals. The natural frequencies and the area under the

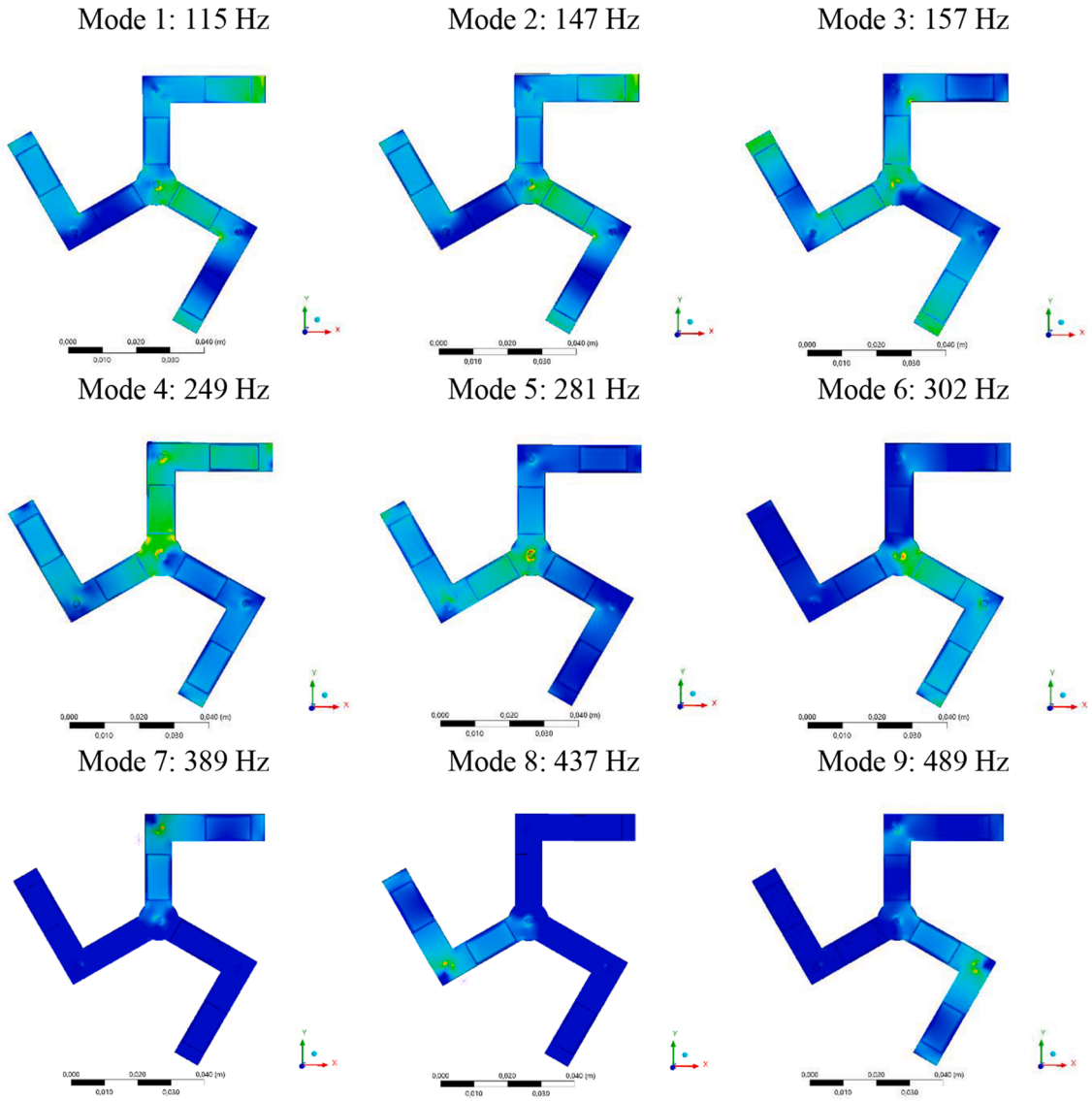

Fig. 6. Modal analysis presenting the first nine natural frequencies and mode shapes of the original MSS harvester showing elastic strain distribution for each vibrational mode.

output power curve are then set as output parameters.

In the first stage of the optimization process, the DOE is used to generate a set of sampling points (design points) that provide discrete results for output parameters in the design space domain. In the second stage, this DOE data is used to fit response surface curves where approximated values of output parameters are represented in terms of input parameters in the design domain. Subsequently, data can be transferred to the *Optimization* component of GDO method, which is a constrained, multi-objective optimization technique to achieve the best designs from a sample set given the objectives and constraints set for parameters. The Multi-Objective Genetic Algorithm (MOGA) is adopted to establish the most suitable candidate points for the optimization problem.

Since a multi-objective problem is solved, the solution is given by a Pareto's frontier, especially where some (or all) of the objectives and constraints are mutually conflicting. In such a case, there is no single point solution that achieves all objectives and restrictions. Instead, the best solutions, denominated as Pareto set, are a group of solutions that optimizes the system according to the objectives and restrictions.

The decision process to determine the most suitable Pareto solution from a sample set is a goal-based and weighted ranking technique. Given N input parameters, M output parameters, and their individual targets, the objectives are described as a single, weighted cost function given by:

$$\phi \equiv \sum_{i=1}^{N} w_i G_i + \sum_{j=1}^{M} w_j Q_j \tag{8}$$

wherew_i are the weights; G_i are normalized objectives for input parameters; Q_j are normalized objectives for output parameters.The normalized objectives metrics can be written as follows:

$$\begin{aligned} G_i &= \left(\frac{|x_t - x|}{x_U - x_L} \right)_i \\ Q_j &= \left(\frac{|y_t - y|}{y_U - y_L} \right)_j \end{aligned} \tag{9}$$

where x is the current value for input parameter i; y is the current value for output parameter j; x_t and y_t correspond to the defined target values; x_L and x_U are the lower and upper values, respectively, for input parameter i; y_L and y_U corresponding to lower and upper bounds, respectively, for output parameter j.

The cost function considers the importance of objectives and con-

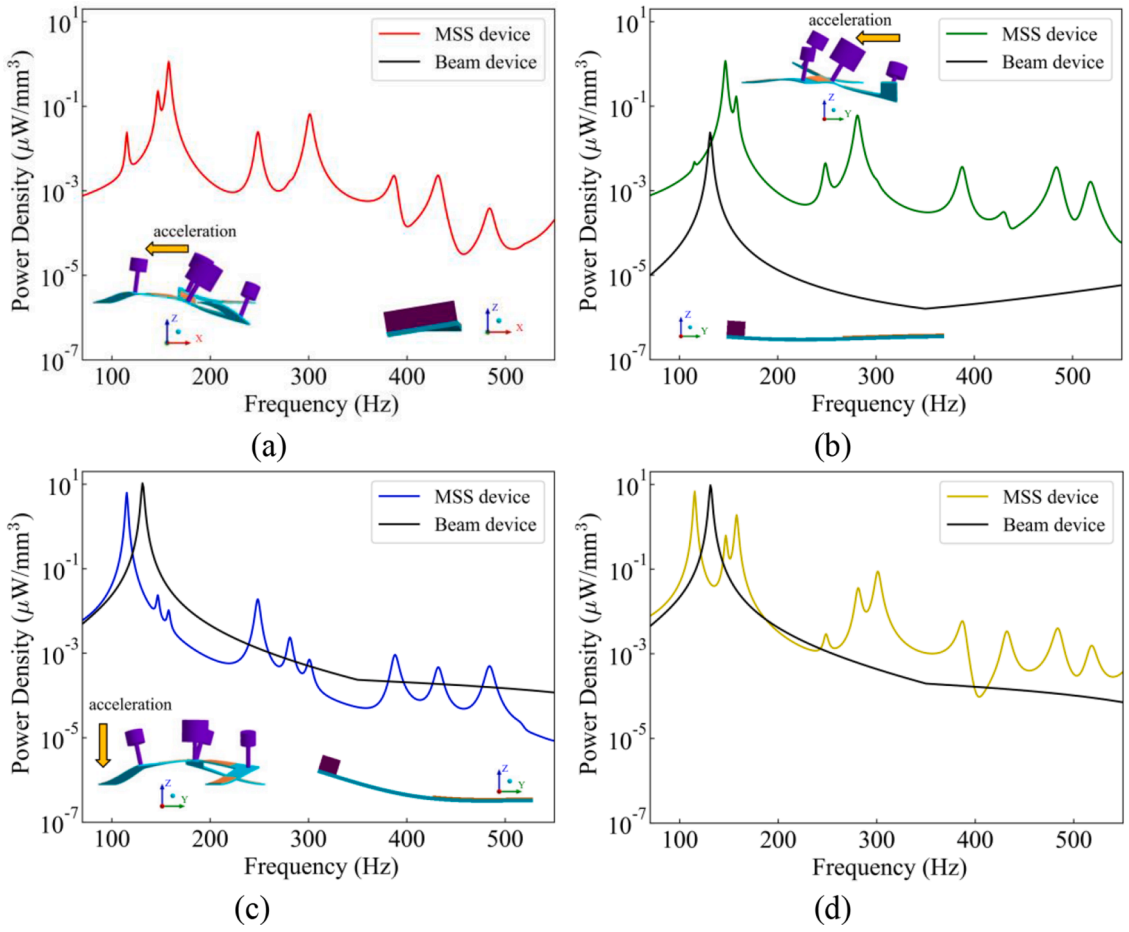

Fig. 7. Comparative analysis of PD frequency response curves for the beam and original MSS devices under 1 *g* amplitude excitation in (a) *x*-axis, (b) *y*-axis, and (c) *z*-axis directions; (d) combination of *x*-, *y*- and *z*-axis excitation.

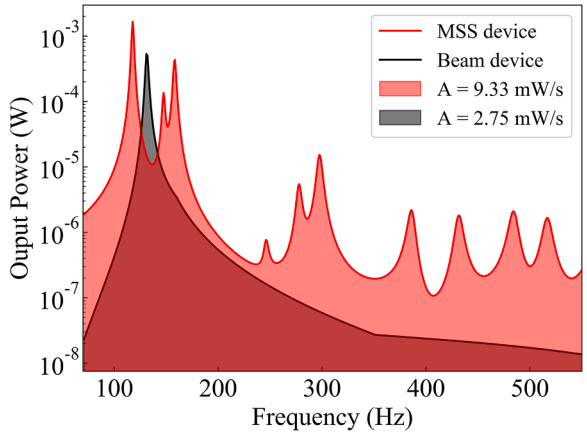

Fig. 8. Output power frequency spectrum for the original MSS and cantilever beam harvester under an excitation in the *x*-, *y*- and *z*-axis directions highlighting the area under the curve metric utilized in the optimization procedure.

straints by assigning weight, which are defined as follows:

$$w_i = w_j = \begin{cases} 1.000, \text{if the importance is Higher} \\ 0.666, \text{if the importance is Default} \\ 0.333, \text{if the importance is Lower.} \end{cases} \quad (10)$$

The decision process sorts the sample set in ascending order using the cost function φ to extract the best candidate points. Since metrics are normalized, the lower the value of φ, the better is the design point with respect to the target objectives and importance. Three best candidate points are selected and, since the optimization procedure is based on the surface response that provides approximate values, the model under investigation is solved for these three candidate points as a verification analysis. Then, the most suitable candidate design is established.

Once the optimized geometry of the system is acquired, the second stage of the optimization procedure obtains the optimal value of resistance load, which represents the electric storage circuit. Harmonic analysis is employed to obtain the steady-state response of the system. The value of resistance load is set as an input parameter and the peak output power as an output parameter. This optimization problem is constructed based in a single-objective function as follows.

Table 2
Geometric dimensions of the best candidate design and resonant frequencies of MSS energy harvesting device.

Parameter	Symbol	Value	Parameter	Symbol	Value
Angle (°)	θ	58	Resonant	RF1	122
	L_0	6	Frequency (Hz)	RF2	133
Rod Length (mm)	L_1	11		RF3	142
	L_2	11		RF4	202
	L_3	11		RF5	244
Pendular Mass	D_0	13		RF6	263
Diameter (mm)	D_1	10		RF7	311
	D_2	9		RF8	339
	D_3	8		RF9	368

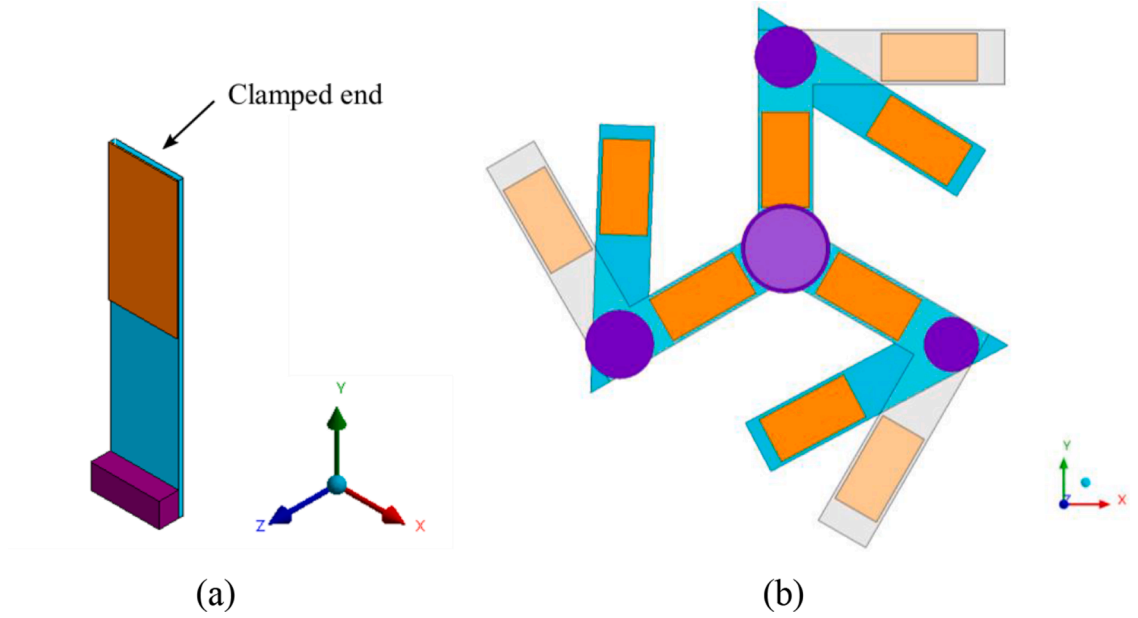

Fig. 9. Comparison of (a) the conventional cantilever beam, (b) the original MSS and the optimized configuration of the MSS energy harvesters.

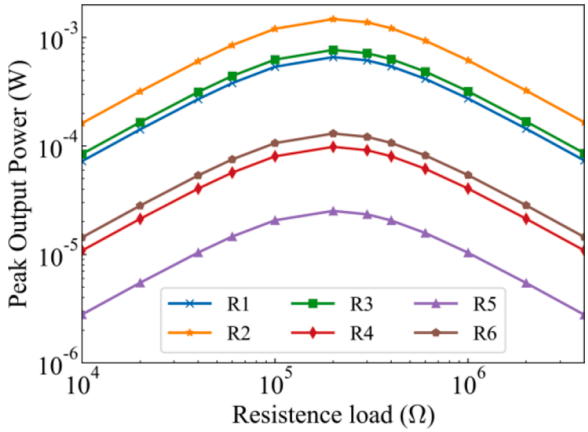

Fig. 10. Peak output power curve as a function of resistance load of each resistor element for the MSS harvester obtained under a base excitation of 1.0 g amplitude acceleration.

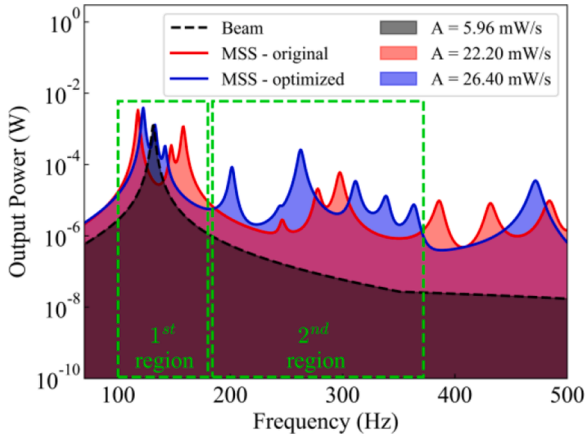

Fig. 11. Comparative analysis between the cantilever beam, the original and optimized MSS devices in terms of the area under the output power curve highlighting two regions with a broadband spectrum.

$$\begin{aligned} &\max_{R} P(R) \\ &\text{subject to the constraint :} \\ &R_L \leq R \leq R_U \end{aligned} \tag{11}$$

where P is the peak output power taken from the frequency response curve; R is the value of resistance load; R_L and R_U are lower and upper bound values for the resistance load.

4. Original design concept

In this section, the proposed multidirectional energy harvester design concept is investigated considering the original design, without optimization. A comparative analysis is performed considering the classical cantilever beam as a performance reference to explore the design concept evolution toward the goal of harness energy from a wideband spectrum from multidirectional excitations.

The conventional energy harvester showed in Fig. 3 is composed of a two-layer sandwich structure with one piezoelectric material (MFC 2814-P2) bonded to a substrate elastic beam of dimensions: 60 × 14 × 1 mm. A tip mass of 2.2 g is placed at the beams' tip to adjustment of resonant frequencies. This device is designed to operate under resonant conditions usually near the first vibrational mode, being suitable for energy harvesting for ambient excitations in its transversal (z-axis) direction.

The original MSS device (Fig. 3) consists of a two-layer sandwich structure, composed of a three L-shaped substrate, six piezoelectric patches, and four pendular masses. The substrate and the inertial pendular masses are made of aluminum and steel alloys, respectively. The macro fiber composite (MFC) material of type MFC0714-P2 operates under d_{31} piezoelectric mode, being used to convert the ambient vibration into electric potential. Table 1 shows geometric dimensions and material properties. The device multimodal characteristic is explored to provide close resonant peaks expanding the operational frequency bandwidth of the system. Additionally, the use of pendular masses allows energy harvesting from multidirectional ambient vibrations, constituting an advantage compared with conventional beam harvesters.

Ambient vibration is transferred to the harvester through a base support with clamped end condition. The base support is modeled by coupling the nodes in the surface located at one substrate ends (Fig. 3). In order to provide uniform electric potentials, the electrodes of

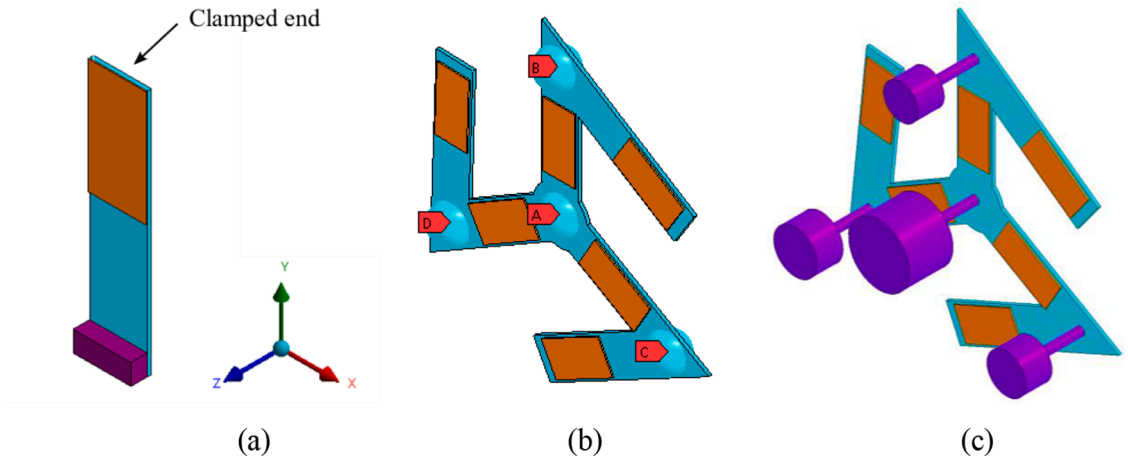

Fig. 12. Schematic representation of (a) cantilever beam, (b) USS and (c) MSS energy harvester.

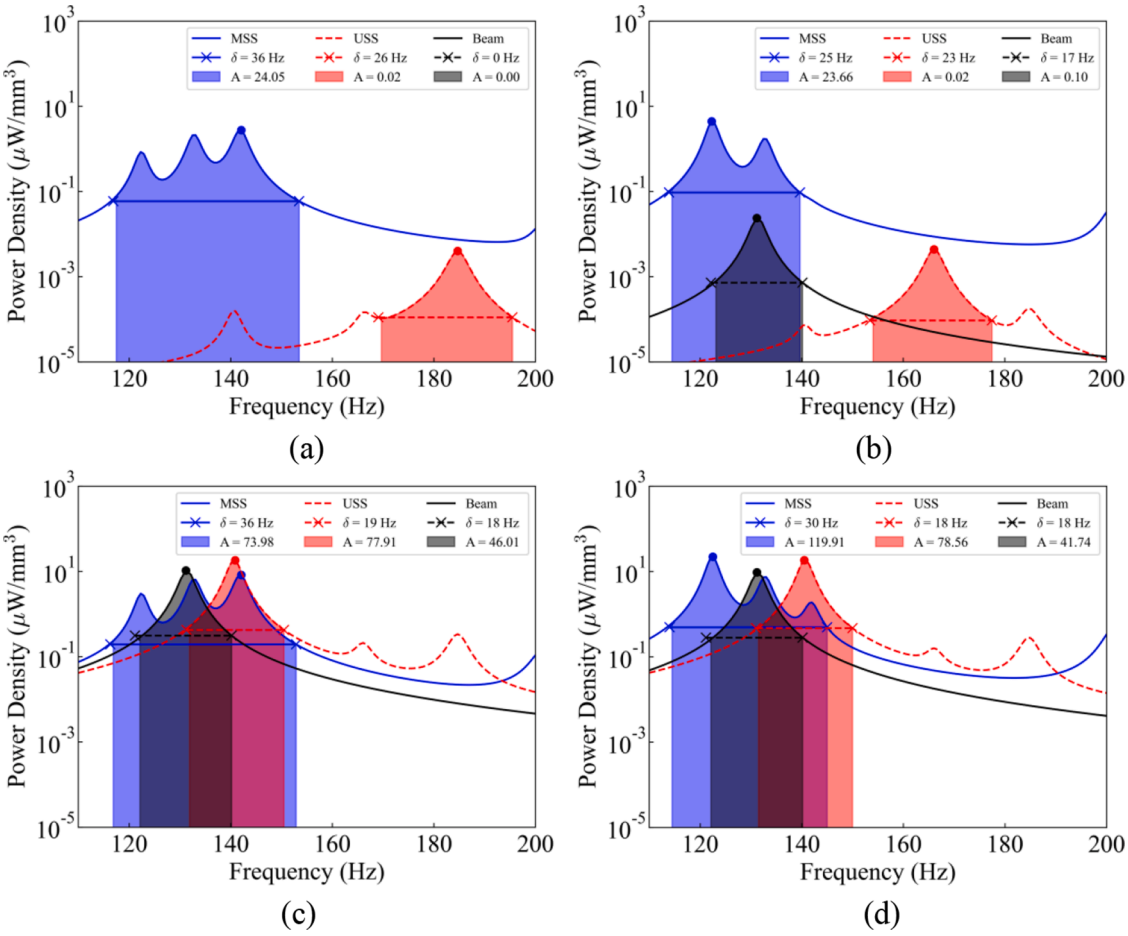

Fig. 13. Frequency response curves of power density under 1 *g* amplitude excitation in (a) *x*-axis, (b) *y*-axis, and (c) *z*-axis directions; (d) combination of *x*-, *y*- and *z*-axis excitation.

piezoelectric elements are emulated by coupling the voltage DoFs on the top and bottom surfaces. The bottom electrode is grounded by assigning a null value and, consequently, the measured electric potential on the top electrode corresponds to the generated electric potential. Fig. 4 shows schematically these applied boundary conditions for the cantilever beam device.

A mesh convergence is carried out by evaluating the skewness and quality factor metrics, and the difference between results of natural frequencies. The mesh is constructed having three elements in thickness for each layer of the substrate and piezoelectric patch, providing a total of 2000 elements for the cantilever-beam and and 30,000 elements for the MSS device, as presented in Fig. 5, that also shows the electronic circuit represented by an electric load resistance.

Initially, a modal analysis is performed to obtain the natural frequencies and mode shapes of the system. A modal damping ratio equal to 2% is adopted. Fig. 6 shows the resonant frequency and relative values of strain distribution for the first nine vibrational modes, which are lined in a frequency range between 100 and 360 Hz. Based on the

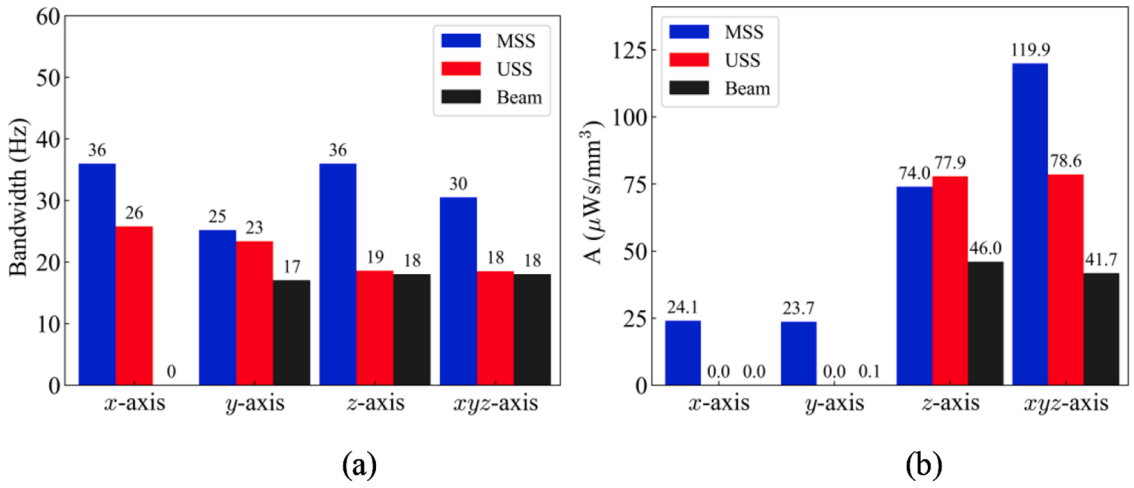

Fig. 14. Comparative analysis of (a) frequency bandwidth (δ) and (b) area under PD curve (A) between the optimized MSS, USS, and cantilever-beam devices.

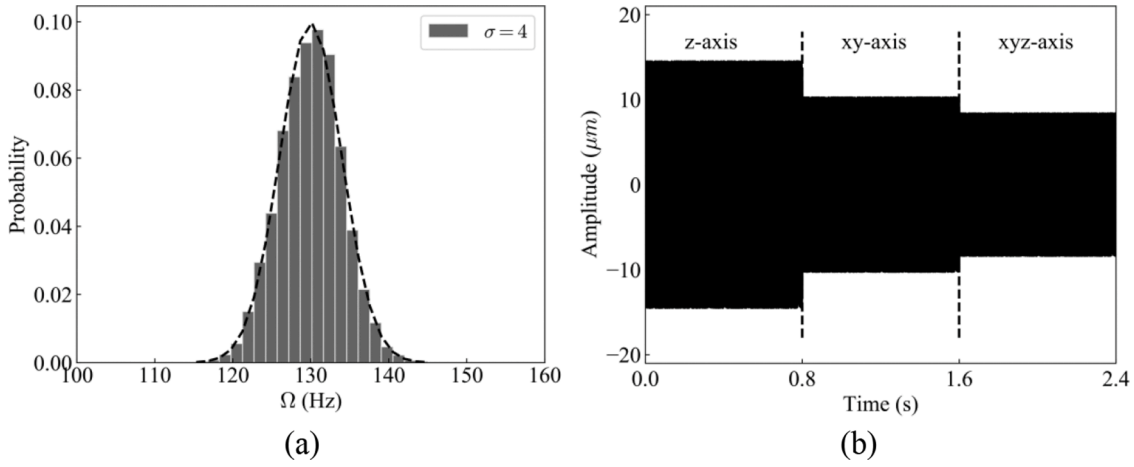

Fig. 15. (a) Histogram of random-frequency excitation presenting Gaussian distribution with a mean value of 130 Hz and standard-deviation of σ = 4, (b) time-history signal of random-frequency excitation with amplitude of u_0 = 14.48 μm.

Table 3
Values of amplitude parameters used to construct the multidirectional time-history excitation.

Excitation direction	Parameters		
First region: *z*-axis	$\alpha_x = 0.0$	$\alpha_y = 0.0$	$\alpha_z = 1.0$
Second region: *xy*-axis	$\alpha_x = 1/\sqrt{2}$	$\alpha_y = 1/\sqrt{2}$	$\alpha_z = 0.0$
Third region: *xyz*-axis	$\alpha_x = 1/\sqrt{3}$	$\alpha_y = 1/\sqrt{3}$	$\alpha_z = 1/\sqrt{3}$

strain distribution, the third mode is the most interesting, followed by the first and second modes, due to higher deformation intensity and, consequently, a bigger capacity to convert electrical potential from the piezoelectric patches. Moreover, the fourth, fifth, and sixth modes present areas with some level of deformation intensity, which could be explored to be converted into electricity. The remaining vibrational modes have less interest since lower intensity is spread in the piezoelectric areas.

The original MSS energy harvester is now investigated under harmonic excitation, considering multidirectional vibration sources. Harmonic analyses are carried out considering a sinusoidal base excitation with $u_0 = a_0/\Omega^2$ displacement amplitude applied at nodes of the base support using $a_0 = 1.0$ g ($\approx$ 9.81 m/s^2) within a frequency range 70 Hz $\leq \Omega \leq$ 550 Hz. Different directions are adopted providing the same energy input for each excitation condition: $u_0 = \sqrt{u_x^2 + u_y^2 + u_z^2}$. Fig. 7 presents the power density considering in-plane ($u_x = u_0$ or $u_y = u_0$), out-of-plane ($u_z = u_0$) and combined ($u_x = u_y = u_z = u_0\sqrt{3}$) vibrations.

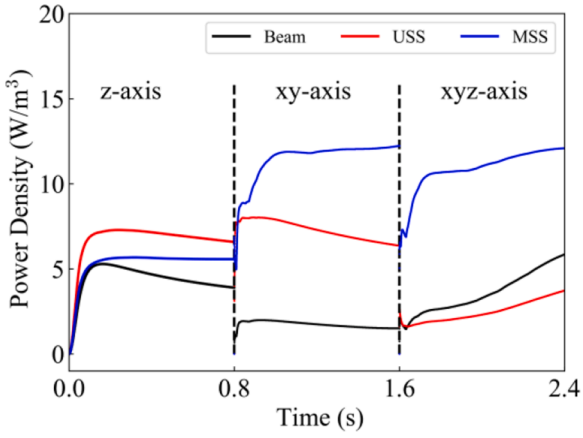

Fig. 16. Time-history response of RMS PD for a multi-direction random-frequency excitation with $\overline{\Omega} = 130$ Hz and σ = 4 Hz; comparative analysis for the beam, USS, and MSS devices.

The system response subjected to an out-of-plane excitation in the z-axis direction is showed in Fig. 7c. The MSS device has the first vibration mode as the predominant one, presenting close peak values of output power compared with the beam device. Valleys are observed between resonant peaks which constitute regions in the frequency spectrum that causes a decrease in the levels of energy harvested. Although this is unavoidable in multimodal systems, the mitigation of these valleys is of special interest in the design of multimodal harvesters. The cantilever-type harvester presents better performance for out-of-plane vibration, operating in its first bending mode (Fig. 7c). The power density response curves for in-plane vibration in the x-axis (Fig. 7a) and the y-axis directions (Fig. 7b) are presented. Higher-order vibration modes become predominant compared with the fundamental mode, presenting improvements regarding the beam device. Lower levels of energy are converted by the beam device for y-axis excitations since the second bending mode is predominant (Fig. 7b) while almost nothing is collected through x-axis direction since a torsional vibrational mode is achieved (Fig. 7a). The power density spectrum for the systems subjected by a combined in-plane and out-of-plane vibration excitation (Fig. 7d) shows that the original MSS energy harvester has an enhanced performance in the entire spectrum for multidirectional excitation.

The MSS piezoelectric device shows potential to harness energy from a multidirectional vibration source, serving as an alternative to the unidirectional sensitivity limitation of conventional single-mode energy harvester devices. The MSS device presents a wider bandwidth compared to the conventional beam device, however, its resonant peak lays in a valley region of the MSS device, as shown in Fig. 7d, which constitutes a drawback. Therefore, further design improvements can be performed to extract energy in a broader frequency spectrum. On this basis, an optimization procedure is employed in the proposed MSS energy harvester design seeking adjusting configurations based on resonant peaks, frequency bandwidth, and output power.

5. Optimized energy harvesting system

This section aims to investigate the optimized MSS device under base excitation in different directions representing diverse conditions of ambient vibrations. The goal is to optimize the harvester based on geometrical and electrical parameters to further improved the system harness capability, establishing the advantages in terms of multidirectional and wideband energy extraction. The system responses are tested considering harmonic and random excitations.

5.1. Optimization procedure

The optimization of the MSS harvester is based on the procedure presented in Section 3.1, considering a design space defined by setting the following upper and lower bound values for each input parameter: $50\,^{\circ} \leq \theta \leq 140\,^{\circ}$, $6 \leq L_0 \leq 12$ mm, $9 \leq L_1 \leq 12$ mm, $L_2 = L_3 = L_1$, $10 \leq D_0 \leq 14$ mm, $4 \leq D_1 \leq 10$ mm, $8 \leq D_2 \leq 11$ mm and $6 \leq D_3 \leq 9$ mm, subject to the restriction, $\omega_g = 10$ Hz. The natural frequencies from modal analysis and the area under the output power curve from harmonic analyses are set as output parameters. Two goals are pursued in the optimization: design the resonant frequencies of the harvester to be spread over the frequency range of 100–500 Hz, while minimizing the gap between successive frequencies; and maximize the area under the output power frequency spectrum. Fig. 8 illustrate this idea by comparing the output power spectrum of the MSS device with the cantilever beam.

Based on results presented in Fig. 7, the following boundaries are assumed: the first, second and third natural frequencies to line in the range of 100–200 Hz; the fourth, fifth and sixth natural frequencies to line in the range of 200–500 Hz; the remaining three natural frequencies to line in the range of 300–500 Hz. Additionally, a target value of 131 Hz is set for the second mode, which is the resonant frequency of the cantilever beam device.

The best candidate point obtained from the RSO procedure is provided in Table 2 together with the nine resonant frequencies. Note that all resonant frequencies line in the desired frequency range. The optimized geometry of MSS device is showed in Fig. 9 together with original MSS and beam devices for comparison proposes.

The second part of the optimization procedure is the determination of the optimal resistance load of the electric circuit. Harmonic analyses are carried out for a base excitation of 1.0 g amplitude acceleration for different values of load resistance to establish the optimal value in terms of maximum output power. Therefore, the peak output power is taken from the frequency spectrum curve for a specific resistance load value. Fig. 10 shows the peak output power as a function of resistance load for each resistor element in the range of 10 kΩ–10 MΩ. The optimal resistance load value is determined as 200 kΩ for both original and optimized MSS harvesters, being used for all simulations. On the other hand, the optimal resistance load for the beam device is 50 kΩ [2].

The effectiveness of the optimization procedure is established by considering the energy harvester devices subjected to time series analysis. Initially, harmonic excitation is of concern building the system response curve for the range of 70–550 Hz, using a base acceleration of 1.0 g amplitude. Fig. 11 shows a comparative analysis of the generated output power spectrum between the cantilever beam and the proposed device, including the MSS original and optimized designs. Two frequency regions are highlighted for lower and higher frequencies. The MSS devices present multiples resonant peaks establishing an advantage compared with cantilever beam device that has only one peak in the desired frequency range. The beam device peak is located around 131 Hz which is a region where the MSS original device has a valley and consequently, the beam presents better performance. This limitation is overcome for the optimized design that presents a broader bandwidth establishing three resonant peaks in the first frequency region. Moreover, five resonant peaks relatively close are obtained in the second frequency range (180–370 Hz) that also allows energy extraction in higher-order frequencies.

5.2. Comparative performance analysis

In this section, the optimized MSS device is investigated considering three-dimensional base excitation representing diverse ambient vibration condition. A comparative analysis is performed for three devices (Fig. 12): the cantilever beam, considered to be a reference case; a unidirectional star-shaped device, without pendular masses (USS); and multidirectional star-shaped device, with pendular masses (MSS). In this regard, the USS device replaces the pendular masses by equally weighted tip masses coupled to the substrate surface, presenting only unidirectional sensitive characteristics.

The output power is not the best metric to compare performance on energy harvesters with different architecture, size, and operation modes. The power density (PD) is a common performance metric used for energy harvester comparison, which is defined as the output power over a unit volume. The PD metric is written as a function of the output power and the volume of piezoelectric material. Fig. 13 presents a comparison of power density spectrum considering excitation in different directions, providing a quantitative analysis regarding the gain in frequency bandwidth. The frequency bandwidth (δ) is estimated by applying the following relation, $P(f_1) = P(f_2) = 0.02P_{max}$, where $\delta = f_2 - f_1$ and $P_{\max}$ is the peak output power taken from the frequency response curve.

Results show that the beam device has only one resonant peak in the frequency range and presents better performance for an out-of-plane vibration in its transversal (z-axis) direction as observed in Fig. 13c. For x-axis direction in-plane excitations, the beam device is operating under torsional vibrational mode and the energy generated by the piezoelectric patches is negligible, as observed in Fig. 13a. For y-axis direction in-plane excitation (longitudinal beam length), the system experiences normal strain as a combination of tension/compression and bending deformation, and consequently, lower levels of electric power

are generated by the piezoelectric patches. The USS harvester presents three resonant peaks in the desired operational frequency range however, they are not close enough to essentially increase the frequency bandwidth of the system. It should be pointed out that the device presents better performance for out-of-plane excitation however, lower levels of PD are generated for in-plane vibration in both x-axis and y-axis directions. The MSS device has three resonant peaks lined in the specified operational frequency range, being close enough to expand system frequency bandwidth. Under the combined in-plane and out-of-plane excitation (Fig. 13d), similar levels of PD peak are noticeable for all the three harvester designs, but the MSS presents wider bandwidth being advantageous for broadband energy harvesting. A quantitative comparative analysis is considered for the harvesters in terms of frequency bandwidth (δ) and parameter A that represents the area under PD curve, with results summarized in Fig. 14. The MSS device presents higher values of parameter A for excitation in multiple directions. For an out-of-plane excitation, the multidirection capability of the MSS device causes an increase of the frequency bandwidth by designing the multimodal system to have close resonant peaks. This constitutes an advantage in terms of energy extraction from broadband frequency spectrum. Therefore, the proposed MSS device allows the exploration of more energy available from ambient excitations providing an interesting alternative to single-mode and unidirectional energy harvesting systems.

Since mechanical energy sources are usually related to multidirectional vibrations with unavoidable uncertainties, the energy harvesters are now investigated considering uncertainties in the ambient excitation, testing their performance through different vibration source conditions. Random ambient vibration excitations are analyzed establishing an energy spread over a wide frequency spectrum. In this regard, fluctuations are investigated considering harmonic excitations with constant amplitude and random-frequency spectrum, defined as $u_b(t) = u_0 \sin(\Omega t)$ where $u_0 = 14.48\ \mu m$ is the base excitation amplitude and the frequency $\Omega = N(\overline{\Omega},\ \sigma)$ corresponds to a Gaussian white noise with a mean value $\overline{\Omega}$ and standard-deviation σ. A histogram with the excitation frequency distribution is presented in Fig. 15a. for a mean value of $\overline{\Omega} =$ 130 Hz and standard-deviation of $\sigma =$ 4 Hz. A time-history signal divided into three regions is built to investigate the multidirectional characteristics of the proposed energy harvesting device. In the first region, a z-axis out-of-plane excitation is considered. Afterward, the second region considers in-plane excitation is assumed simultaneously in the x- and y-axis directions. Finally, the third region considers a multidirectional excitation assuming a combination of in-plane and out-of-plane excitations (x-, y- and z-axis directions). Fig. 15b presents the multidirectional time-history signal for the random-frequency base excitation, using the relations as provided in Table 3: $u_x = \alpha_x u_0$, $u_y = \alpha_y u_0$ and $u_z = \alpha_z u_0$. This is done to provide the same energy input to the harvester device for excitation in different directions by respecting the following relation: $u_0 = \sqrt{u_x^2 + u_y^2 + u_z^2}$.

Transient simulations are carried out during 2.4 s for all energy harvesting devices. A comparative analysis of RMS power density is presented in Fig. 16. Results show that for the out-of-plane vibration (z-axis direction), the beam device presented worse performance when compared with both the USS and the MSS devices due to the broadband spectrum characteristic of the excitation. Under this condition, the USS device showed higher levels of PD compared with the proposed MSS device. This can be attributed to the tip masses being close to the substrate which causes higher oscillations of the structure and therefore, more energy is generated by the piezoelectric patches. For the in-plane vibration (xy-axis direction), the MSS device shows the best performance compared with the USS device providing higher levels of PD. Moreover, in the third region where a combination of in-plane and out-of-plane vibration is considered, the MSS device showed to be advantageous in terms of PD in comparison with the remaining device configurations. Under this condition, the beam device is more efficient than the USS device.

An important aspect to be pointed out is the influence of the ambient vibration conditions in the performance of the MSS device. Although the strategy of using pendular masses to extract energy from multidirectional excitations showed to be interesting, it needs to be analyzed with attention. The pendular mass devices can add additional damping to the system that attenuates vibration energy, reducing the energy harvesting capacity for long term extraction. Besides, pendulum mass can work as a vibration absorber, attenuating the structure vibration, which also reduce the energy harvesting capacity. These aspects are especially important for harnessing energy efficiently. Therefore, the proposed MSS energy harvester device shows potential to extract energy from a broad bandwidth frequency spectrum, allowing a better exploration of energy available from ambient excitations. Nevertheless, a careful design of the device is necessary considering either the device or the ambient vibration characteristics. This paper presented a proof of concept of the idea, but a complete dynamical analysis of the idea should be carried out for specific applications.

6. Conclusions

A multidirectional and multimodal piezoelectric energy harvesting device is proposed, designed, optimized and investigated with the purpose to extract energy from multidirectional and broadband ambient vibration sources. The proposed multidirectional star-shaped (MSS) device utilizes inertial pendular masses with two goals: extract ambient energy from multidirections; and tune the resonant frequencies by carefully changing the weight of the pendular masses. The harvester system analysis is performed employing the finite element method using ANSYS Workbench. Modal and harmonic simulations are conducted, respectively to set resonant frequencies in the desired frequency range and to obtain the system response in the steady-state regime. An optimization procedure is employed pursuing geometric and electric designs. Initially, a parametric study is performed to design the system to achieve as many resonant frequencies as possible in the desired operational frequency range and with close enough resonant peaks, enabling energy harvesting with broadband spectrum. Afterward, the optimal value of the electric resistance load associated with the electronic circuit is obtained aiming at maximizing the output power.

In order to establish the advantages of the optimized MSS device performing a comparative analysis with the conventional cantilever beam design that serves as a reference case of single-mode energy harvester. Besides, the classical cantilever-type harvester, the unidirectional star-shaped (USS) device, without pendular masses, is considered as reference performance cases of a multimodal device with unidirectional sensitivity to ambient excitations. Harmonic and random excitations are investigated for in-plane and out-of-plane vibration and results show that the proposed device presents performance advantages in terms of power density, broadband frequency spectrum and multidirectional excitation capability compared with conventional energy harvesters. A proof of concept of the idea is presented but it should be highlighted that the pendular mass can either introduce extra dissipation or work as an energy absorber, which can reduce energy harvesting capacity. In this regard, the energy harvester design should pay attention in these aspects for the specific case treated Eqs. (1)–((11)).

Declaration of Competing Interest

The authors declare that they have no conflict of interest.

Acknowledgements

The authors would like to acknowledge the support of the Brazilian Research Agencies CNPq, CAPES and FAPERJ.

References

[1] Allik H, Hughes TJ. Finite element method for piezoelectric vibration. Int J Numer Methods Eng 1970;2(2):151–7.
[2] Caetano VJ, Savi MA. Multimodal pizza-shaped piezoelectric vibration-based energy harvesters. J Intell Mater Syst Struct 2021;32(20):2505–28.
[3] Erturk A, Hoffmann J, Inman DJ. A piezomagnetoelastic structure for broadband vibration energy harvesting. Appl Phys Lett 2009;94(25):254102.
[4] Erturk A, Inman DJ. On mechanical modeling of cantilevered piezoelectric vibration energy harvesters. J Intell Mater Syst Struct 2008;19(11):1311–25.
[5] Erturk A, Inman DJ. A distributed parameter electromechanical model for cantilevered piezoelectric energy harvesters. J Vib Acoust 2008;130(4).
[6] Erturk A, Inman DJ. Issues in mathematical modeling of piezoelectric energy harvesters. Smart Mater Struct 2008;17(6):065016.
[7] Erturk A, Inman DJ. An experimentally validated bimorph cantilever model for piezoelectric energy harvesting from base excitations. Smart Mater Struct 2009;18 (2):025009.
[8] Erturk A, Renno JM, Inman DJ. Modeling of piezoelectric energy harvesting from an *L*-shaped beam-mass structure with an application to UAVs. J Intell Mater Syst Struct 2009;20(5):529–44.
[9] Fattahi I, Mirdamadi HR. A novel 3D skeletal frame topology for energy harvesting systems. Microelectron J 2019;83:6–17.
[10] Fattahi I, Mirdamadi HR. A novel multimodal and multidirectional energy harvester by asymmetric 3D skeletal frame structures. J Braz Soc Mech Sci Eng 2020;42(274):1–14.
[11] Ferrari M, Ferrari V, Guizzetti M, Marioli D, Taroni A. Piezoelectric multifrequency energy converter for power harvesting in autonomous microsystems. Sens Actuators A Phys 2008;142(1):329–35.
[12] Giri AM, Ali SF, Arockiarajan A. Dynamics of symmetric and asymmetric potential well-based piezoelectric harvesters: a comprehensive review. J Intell Mater Syst Struct 2020;32(17):1881–947.
[13] Hung CF, Chung TK, Yeh PC, Chen CC, Wang CM, Lin SH. A miniature mechanical-piezoelectric-configured three-axis vibrational energy harvester. IEEE Sens J 2015; 15(10):5601–15.
[14] Johnson TJ, Charnegie D, Clark WW, Buric M, Kusic G. Energy harvesting from mechanical vibrations using piezoelectric cantilever beams. Smart Structures and Materials 2006: Damping and Isolation, 6169. International Society for Optics and Photonics; 2006. p. 61690.
[15] Kim IH, Jung HJ, Lee BM, Jang SJ. Broadband energy-harvesting using a two degree-of-freedom vibrating body. Appl Phys Lett 2011;98(21):214102.
[16] Kim J, Dorin P, Wang KW. Vibration energy harvesting enhancement exploiting magnetically coupled bistable and linear harvesters. Smart Mater Struct 2020;29 (6):065006.
[17] Li X, Yu K, Upadrashta D, Yang Y. Multi-branch sandwich piezoelectric energy harvester: mathematical modeling and validation. Smart Mater Struct 2019;28(3): 035010.
[18] Li X, Yu K, Upadrashta D, Yang Y. Comparative study of core materials and multi-degree-of-freedom sandwich piezoelectric energy harvester with inner cantilevered beams. J Phys D Appl Phys 2019;52(23):235501.
[19] Lu ZQ, Chen J, Ding H, Chen LQ. Two-span piezoelectric beam energy harvesting. Int J Mech Sci 2020;175:105532.
[20] Ng TH, Liao WH. Feasibility study of a self-powered piezoelectric sensor. Smart Structures and Materials 2004: Smart Electronics, MEMS, BioMEMS, and Nanotechnology, 5389. International Society for Optics and Photonics; 2004. p. 377–88.
[21] Ng TH, Liao WH. Sensitivity analysis and energy harvesting for a self-powered piezoelectric sensor. J Intell Mater Syst Struct 2005;16(10):785–97.
[22] Panyam M, Daqaq MF. Characterizing the effective bandwidth of tri-stable energy harvesters. J Sound Vib 2017;386:336–58.
[23] Rezaei M, Talebitooti R. Wideband PZT energy harvesting from the wake of a bluff body in varying flow speeds. Int J Mech Sci 2019;163:105135.
[24] Rezaei M, Takebitooti R, Friswell MI. Efficient acoustic energy harvesting by deploying magnetic restoring force. Smart Mater Struct 2019;28(10):105037.
[25] Shahruz SM. Design of mechanical band-pass filters for energy scavenging. J Sound Vib 2006;292(3-5):987–98.
[26] Sodano HA, Park G, Inman DJ. Estimation of electric charge output for piezoelectric energy harvesting. Strain 2004;40(2):49–58.
[27] Su WJ, Zu J. An innovative tri-directional broadband piezoelectric energy harvester. Appl Phys Lett 2013;103(20):203901.
[28] Suresh K, Shankar K, Sujatha C. A novel passive mechanism to improve power ouput in 2DOF piezoelectric vibration energy harvester. Smart Mater Struct 2019; 28(11):15016.
[29] Tang L, Yang Y. A multiple-degree-of-freedom piezoelectric energy harvesting model. J Intell Mater Syst Struct 2012;23(14):1631–47.
[30] Tang L, Yang Y. A nonlinear piezoelectric energy harvester with magnetic oscillator. Appl Phys Lett 2012;101(9):094102.
[31] Tang L, Yang Y, Soh CK. Toward broadband vibration-based energy harvesting. J Intell Mater Syst Struct 2010;21(18):1867–97.
[32] Upadrashta D, Yang Y. Trident-shaped multimodal piezoelectric energy harvester. J Aerosp Eng 2018;31(5):04018070.
[33] Wang G, Wu H, Liao WH, Cui S, Zhao Z, Tan J. A modified magnetic force model and experimental validation of a tri-stable piezoelectric energy harvester. J Intell Mater Syst Struct 2020;31(7):967–79.
[34] Wang H, Tang L. Modeling and experiment of bistable two-degree-of-freedom energy harvester with magnetic coupling. Mech Syst Signal Process 2017;86: 29–39.
[35] Wu H, Tang L, Yang Y, Soh CK. A novel two-degrees-of-freedom piezoelectric energy harvester. J Intell Mater Syst Struct 2013;24(3):357–68.
[36] Yu Q, Yang J, Yue X, Yang A, Zhao J, Zhao N, Wen Y, Li P. 3D, wideband vibro-impacting-based piezoelectric energy harvester. AIP Adv 2015;5(4):047144.
[37] Zhao Y, Qin Y, Guo L, Tang B. Modeling and experiment of a V-shaped piezoelectric energy harvester. Shock Vib 2018;2018:7082724. Article.
[3888] Zhang J, Qin L. A tunable frequency up-conversion wideband piezoelectric vibration energy harvester for low-frequency variable environment using a novel impact- and rope-driven hybrid mechanism. Appl Energy 2019;240:26–34.
[39] Zhou Z, Qin W, Zhu P. Improve efficiency of harvesting random energy by snap-through in a quad-stable harvester. Sens Actuators A Phys 2016;243:151–8.
[40] Zhou Z, Qin W, Zhu P. Harvesting performance of quad-stable piezoelectric energy harvester: modeling and experiment. Mech Syst Signal Process 2018;110:260–72.
[41] Zou D, Liu G, Rao Z, Tan T, Zhang W, Liao W-H. Design of a multi-stable piezoelectric energy harvester with programmable equilibrium point configurations. Appl Energy 2021;302:117585.
[42] Zhu D, Tudor MJ, Beeby SP. Strategies for increasing the operating frequency range of vibration energy harvesters: a review. Meas Sci Technol 2009;21(2):022001.